Terahertz Radiation from a Nonlinear Slab Traversed by an Optical Pulse

N. N. Zinov'ev,[1,2,*] A. S. Nikoghosyan,[3] and J. M. Chamberlain[1]

[1]*Department of Physics, University of Durham, Durham DH1 3LE, United Kingdom*
[2]*A. F. Ioffe Physical Technical Institute, 194021 St. Petersburg, Russia*
[3]*Department of Microwave Engineering, Yerevan State University, Yerevan 375025, Armenia*

(Received 28 June 2006; published 24 January 2007)

We report on the theoretical calculations considering collinear electromagnetic radiation at the propagation of an optical pulse through a slab of nonlinear material. Calculated waveforms of the radiated field fit well to the experimental dependencies showing the remarkable similarities between the radiation at nonlinear wave interaction and the radiation phenomena of moving external charges, similarly to discussed in the Tamm Problem and transition radiation of moving external charges.

DOI: 10.1103/PhysRevLett.98.044801 PACS numbers: 41.60.−m, 42.65.Ky

Nonlinear wave conversion (NLWC) [1,2] interprets the generation of an optical wave as the result of interference in the bulk of a sample of two partial waves: the inhomogeneous wave (IHW), and the homogeneous wave (HW). This may be tentatively extended to a difference frequency and the interaction of wave packets, for which HW is the bunch of waves grouping around the conversion frequency ω with the wave vectors $k_\omega = \omega/c(\omega)$. IHW is the wave packet with the same frequencies $\omega = \Delta\omega_p$, but with wave vectors $k_{\omega_p} - k_{\omega_p+\Delta\omega_p} \sim \omega/v_g(\omega_p)$, where $\Delta\omega_p$ is the bandwidth of the pump. Constructive interference of IHW and HW occurs on the scale of the coherence length $L_{\mathrm{coh}}^{\mathrm{FW}}$ where the phase matching condition is met [3,4]. In practice, because of dispersion and wave vector mismatch, phase matching is rarely achieved over a large length scale, at least for a broad band of frequencies. So far, a considerable number of papers published on nonlinear interactions of wave packets have used the NLWC model to interpret their results, e.g., [5–9]. On the other hand, the generation of high frequency electromagnetic radiation from the passage of a short optical pulse through a nonlinear medium has been suggested [10] by analogy with the moving charge radiation phenomena, Vavilov-Cherenkov radiation (VCR) and transition radiation (TR) [11]. It is known from [12–14] that VCR hardly couples into free space because of Cherenkov angle normally exceeds the angle of total internal reflection. Therefore, in this Letter we consider only collinear mechanism of terahertz (THz) radiation.

The NLWC model was not called into question until the publication of [15] where a new effect was found experimentally: a twin pulse of THz radiation generated from the nonlinear conversion of a single optical pulse in an electro-optic crystal, and tentatively attributed to a type of radiation emanating from boundaries. Such twin pulses, however, may be alternatively interpreted within the NLWC model by associating THz pulses with the HW and IHW. Because of dispersion the HW and IHW packets "walk-off" with different velocities, c, v_g, respectively. Then the difference Δt in the arrival time for HW and IHW pulses at the end of crystal considered as the near field is $\Delta t = L/c - L/v_g$.

This ambiguity, associated with the application of NLWC and TR models, calls for a reappraisal of the theoretical foundation of the generation of radiation in nonlinear media. Although both models (for different reasons) require nonlinear coupling of pump fields, the physics of the emission mechanisms are distinctively different. To analyze THz generation in nonlinear materials we use frequency-time domain analysis of radiation resulting from the propagation of a short pump pulse through a slab of nonlinear medium of thickness L and under the condition of arbitrary wave vector mismatch. The analysis begins from the set of equations for the electric component of the THz field in time domain, $\mathbf{E}(\mathbf{r}, t)$ including the wave equation:

$$\nabla^2\mathbf{E}(\mathbf{r}, t) - \frac{1}{c_0^2}\int_{-\infty}^{+\infty} dt'\epsilon(t-t')\frac{\partial^2}{\partial t'^2}\mathbf{E}(\mathbf{r}, t') = \mu_0\frac{\partial^2\mathbf{P}^{\mathrm{NL}}(\mathbf{r}, t)}{\partial t^2} + \nabla\cdot[\nabla\cdot\mathbf{E}(\mathbf{r}, t)] \quad (1)$$

and the Poisson equation

$$\epsilon_0\int_{-\infty}^{+\infty} dt'\epsilon(t-t')\nabla\cdot\mathbf{E}(\mathbf{r}, t') = -\nabla\cdot\mathbf{P}^{\mathrm{NL}}(\mathbf{r}, t), \quad (2)$$

where

$$\mathbf{P}^{\mathrm{NL}}(\mathbf{r}, t) = \epsilon_0\int_{-\infty}^{+\infty} dt'\hat{\chi}^{(2)}(t-t'):\mathbf{E}_p(\mathbf{r}, t')\mathbf{E}_p^*(\mathbf{r}, t'). \quad (3)$$

The first item in the right-hand side (rhs) of (1) is the time derivative of nonlinear term of the displacement current $\mathbf{J}_d^{\mathrm{NL}}$. It can be represented in the form of the flux of polarization charge: $\mathbf{J}_d^{\mathrm{NL}}(\mathbf{r}, t) = \partial\mathbf{P}^{\mathrm{NL}}(\mathbf{r}, t)/\partial t = \nabla\cdot\mathbf{P}^{\mathrm{NL}}(\mathbf{r}, t)\cdot\partial\mathbf{r}/\partial t = -\rho_d(\mathbf{r}, t)\mathbf{v}$, where $\mathbf{v}$ is the velocity of polarization charge. For a propagating wave packet, $\mathbf{v}$ is the group velocity. This description resembles the familiar statement in the theory of radiation from moving charges [11]. In this case, instead of an external uniformly moving free charge, a polarization charge is formed in the medium due to nonlinear coupling of fields. Then (1) and (3)

describe radiation phenomena of a moving polarization charge with density $\rho_d = -\nabla \cdot \mathbf{P}^{\mathrm{NL}}$. In the slab, the charge is created at $z = 0$ and instantaneously accelerated upon entry of the pump pulse into slab. The charge then moves uniformly across the slab. Finally, the polarization charge is instantaneously decelerated and extinguished at $z = L$ upon exit of the pump pulse from the slab emitting a second burst of radiation. The situation is analogous to the Tamm problem of the start-stop motion of a free charge [16,17]. For collinear and anticollinear radiation at the normal incidence of pump the problem has axial symmetry along the z axis. The wave front of the pump field within the slab volume can be considered as nearly plane, and constrained within an aperture determined by the beam diameter S_0. For a short optical pulse, we use a slowly varying amplitude approximation representing the pump electric field in the rhs of (3) as the product of the Gaussian pulse envelope and the plane carrier wave at the frequency ω_0: $\mathbf{E}_p(z,t) = \frac{1}{2}\mathbf{e}_x E_0 \exp[-(t - z/v_g)^2(4\tau_p^2)^{-1}]\exp\{i[\omega_0 t - k(\omega_0)z]\} + \text{c.c.}$, where v_g is the group velocity of the pump wave packet: $v_g = c_0[n(\omega_0) + \omega_0 dn(\omega_0)/d\omega_0]^{-1}$, τ_p is pulse FWHM [7]. The solution of (1)–(3) in the slab sums up the multiple reflections of the THz radiation obtained from a single flight of the pump pulse. Then, after some algebra and Fourier transforms, (1) and (3) are reduced to an ordinary differential equation in the form

$$\frac{d^2E_x(z,\omega)}{dz^2} + \frac{\omega^2}{c^2}E_x(z,\omega) = -S(\omega)\exp\left(i\frac{\omega}{v_g}z\right), \quad (4)$$

where $S(\omega) = (\omega^2/c_0^2)\sqrt{2\pi}\hat{\chi}^{(2)}E_0^2\tau_p \exp(-\omega^2\tau_p^2/2)$, $c = c_0/\sqrt{\epsilon(\omega)} = c_0/n(\omega)$. The general solution of (4) is

$$E_x(z,\omega) = C_1\exp\left(i\frac{\omega}{c}z\right) + C_2\exp\left(-i\frac{\omega}{c}z\right) + \frac{L_{\mathrm{coh}}^{\mathrm{FW}}L_{\mathrm{coh}}^{\mathrm{BW}}S(\omega)}{\pi^2}\exp\left(i\frac{\omega}{v_g}z\right). \quad (5)$$

Here C_1 and C_2 are the integration constants, $L_{\mathrm{coh}}^{\mathrm{FW}}(\theta,\omega) = \pi/|\Delta k_{\mathrm{FW}}|$, $\Delta k_{\mathrm{FW}} = (\omega/v_g)|(1 - v_g/c)|$ and $L_{\mathrm{coh}}^{\mathrm{FW}} \equiv L_{\mathrm{coh}}^{\mathrm{FW}}(\theta = 0,\omega)$ and $L_{\mathrm{coh}}^{\mathrm{BW}} = \pi/\Delta k_{\mathrm{BW}}$, $\Delta k_{\mathrm{BW}} = (\omega/v_g)\times[1 + (v_g/c)]$. $L_{\mathrm{coh}}^{\mathrm{FW}}(\omega)$ is the formation or coherence length characterizing the efficiency of the emission process at wave conversion in the forward direction [18]. $L_{\mathrm{coh}}^{\mathrm{BW}}(\omega)$ is the coherence length for backward THz emission. The first two terms in (5) represent the radiation field and the third term describes the field of the polarization charge. For a transverse field, the boundary conditions require the tangential components of electric and magnetic fields to be continuous at the interfaces $z = 0$ (input boundary of the nonlinear slab) and at $z = L$ (output boundary of the nonlinear slab) [19]. The solution (5) is matched with the solutions of homogeneous wave equation in free space, the left-hand side of (4), propagating backward and forward. Finally, the expressions for THz field amplitudes outside the slab for forward propagating wave, $z = L+$ and backward propagating wave, $z = 0-$ are given by

$$E_x(L+,\omega) = -\frac{c_0}{\pi^2 v_g}\frac{L_{\mathrm{coh}}^{\mathrm{FW}}L_{\mathrm{coh}}^{\mathrm{BW}}S(\omega)}{(c - c_0)^2\exp(i\omega L/c) - (c + c_0)^2\exp(-i\omega L/c)} \times \{(c + c_0)(c + v_g)\exp[-i\omega L(1/c - 1/v_g)] - (c - c_0)(c - v_g)\exp[i\omega L(1/v_g + 1/c)] - 2c(v_g + c_0)\} \quad (6)$$

$$E_x(0-,\omega) = \frac{c_0}{\pi^2 v_g}\frac{L_{\mathrm{coh}}^{\mathrm{FW}}L_{\mathrm{coh}}^{\mathrm{BW}}S(\omega)}{(c - c_0)^2\exp(i\omega L/c) - (c + c_0)^2\exp(-i\omega L/c)} \times \{2c(v_g - c_0)\exp(i\omega L/v_g) + (c + c_0)(c - v_g) \times \exp(-i\omega L/c) - (c + v_g)(c - c_0)\exp(i\omega L/c)\}, \quad (7)$$

respectively. The spatial distribution of light emitted into a far remote zone in free space can be retrieved after solving the diffraction integral [20]. This describes the time domain waveform at a remote distance r, diffracted from emitting apertures of the size S_0 at both input and output surfaces, (6) and (7):

$$E_{\mathrm{THz}}(t) = E_x(r,t) = \frac{1}{(2\pi)^2 c_0}\int_{S_0}\frac{\cos(\mathbf{n},\mathbf{r})}{r}\frac{d}{dt}E_x\left(z = L+, t - \frac{r}{c_0}\right)dS_0, \quad (8)$$

where $E_x(z = L+, t - r/c_0)$ is the inverse Fourier transform of $E_x(L+,\omega)$. Similarly, the THz field emitted by the slab in the backward direction is found from (8) using $E_x(z = 0-,\omega)$ instead of $E_x(z = L+,\omega)$.

To compare adequately the results of numerical calculations with our experimental data, we compute theoretical waveforms taking into account the instrumental factors introduced by the electro-optic sampler [21]. The detected THz waveform, $S_{\mathrm{THz}}(\tau)$, is

$$S_{\mathrm{THz}}(\tau) = \frac{\pi\epsilon_0}{c}\int_{-\infty}^{\infty}E_{\mathrm{THz}}(t - \tau)f(t)dt. \quad (9)$$

The instrumental factor $f(t)$ in (9) results from the wave vector mismatch between THz and probe pulses in the electro-optic material. For a nearly phase matching in the detector, it is approximated by the relationship [22]

$$f(\omega) = \frac{\pi\epsilon_0\omega_0^2}{c_0 k(\omega_0)}\exp[-2\beta(\omega_0)L]t_{12}(\omega)C_{opt}(\omega) \times \frac{\exp[i\Delta k(\omega,\omega_0)L] - 1}{i\Delta k(\omega,\omega_0)L}, \quad (10)$$

where $k(\omega_0)$ is the real part of the complex wave vector κ; $\beta(\omega_0)$ is the attenuation coefficient;

$\kappa(\omega) = k(\omega) + i\beta(\omega) = (\omega/c_0)n(\omega)$; $t_{12}(\omega) = 2/[n(\omega) + 1]$ is the Fresnel coefficient for THz radiation at a frequency ω crossing air-electro-optic detector crystal boundary; and $C_{\text{opt}}(\omega)$ is the autocorrelation function of the probe pulse electric field. All material parameters necessary for calculations are taken from [23,24].

The waveform of THz radiation calculated and measured from a 1 mm slab of $LiNbO_3$ in free space is shown in Fig. 1. The theoretical waveform fits quite well with the experimental time dependence. The THz waveform consists of several separated pulses. Two leading pulses, TA and TB, (curve 1 and 2, Fig. 1), represent THz radiation emitted during a single flight of the pump pulse; and are consistent with the observation made in [15]. Prefix "T" here indicates the transmission geometry, i.e., THz radiation emitted from the slab in the forward direction. Each pulse starts with intensive bipolar oscillations defining the overall shape of the spectral envelope [25]. Figure 2 plots the fan diagram of pulse positions as a function of slab thickness. The position of pulse TA follows the time of flight of the pump pulse, $t_A = Ln_{\text{opt}}(\omega_0)/c_0$. The temporal position of the pulse TB corresponds to $t_B = Ln_{\text{THz}}/c_0$; that is, the time of flight of the THz radiation pulse across the slab. The relative time of flight between pulses TA and TB is $\Delta t_{A\text{-}B} = L(n_{\text{THz}} - n_{\text{opt}})/c_0$. As stated above, these data themselves do not deliver conclusive evidence on the spatial location of the source regions of TA and TB pulses. In search of such proof we turn to the analysis of other properties of radiation that so far have not been addressed.

The amplitude dependence on thickness for forward emitted radiation, shown in Fig. 2, demonstrates linear growth of the main THz pulse amplitude at thicknesses $L < L_{\text{coh}}^{\text{FW}}$. At a certain thickness, corresponding to the onset of wave vector mismatch, the main pulse splits into two labeled as TA and TB pulses. The amplitude of pulse TA saturates with L and remains largely constant irrespective of further increase of slab thickness. Unlike pulse TA, the amplitude of pulse TB strongly falls with L. This may be regarded as a signature of strong attenuation and broadening of the pulse TB inside the slab. To identify a convincing proof we address the comparison of the properties of TA and TB pulses and their echo replicas, the pulses TA′ and TB′ following the leading pair TA-TB. The key significance of the data extracted from the properties of echo replicas is motivated by the idea that, for spatially separated sources (TR model), the echo replicas should show characteristic modifications of properties; whereas, for the pulses generated within the same volume adjacent to the input surface (NLWC model), the echo replicas should have, at least, the same structure and amplitude ratio. Moreover, if, as suggested in [1], the so-called IHW does indeed represent a real propagating wave (created by nonlinear conversion along with HW), it must keep its "extraordinary" properties. These are the following: the frequency is equal to the conversion frequency ω; and the complex wave velocity v_g is equal to that of pump pulse. From Fig. 2, showing the fan diagram of arrival times for the main pulses and their reflection replicas, we can see that time positions for the TB′ replica behave consistently with the properties of the TB pulse. Being reflected sequentially from the output and input interfaces, the pulse TB′ acquires a round trip delay $2Ln_{\text{THz}}/c_0$ in addition to the direct arrival time $t_{B'} = 3Ln_{\text{THz}}/c_0$. The arrival time of flight for the TA′ pulse, $t_{A'}$, includes the time of flight of TA, Ln_{opt}/c_0 accomplished with a round trip

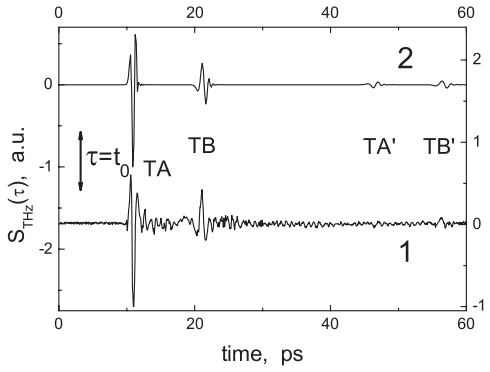

FIG. 1. Comparison of experimental (*curve 1*) and theoretical (*curve 2*) THz waveforms forwardly emitted from the slab of $LiNbO_3$ of 1 mm thickness. Pulses labeled TA-TB, and TA′-TB′ corresponds to forward emitted THz radiation and their first round trip echo-replicas, respectively. Mark t_0 shows the time corresponding the entry of pump pulse in nonlinear slab ($z = 0$).

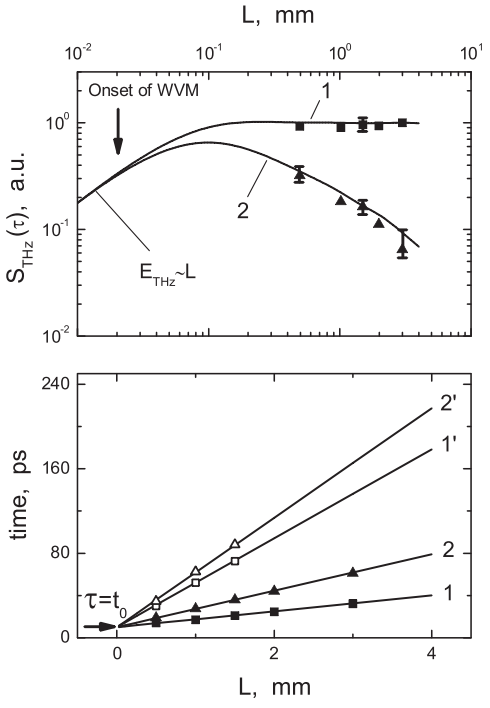

FIG. 2. Bottom: Fan diagram showing positions of peaks TA (1), TB (2), TA′ (1′) and TB′ (2′) as functions of slab thickness L. Top: Dependencies of THz field peak amplitude on slab thickness for pulse TA (1) and pulse TB (2). Experimental points are shown by squares and triangles. Solid curves 1, 2, 1′, and 2′ show theoretical dependencies.

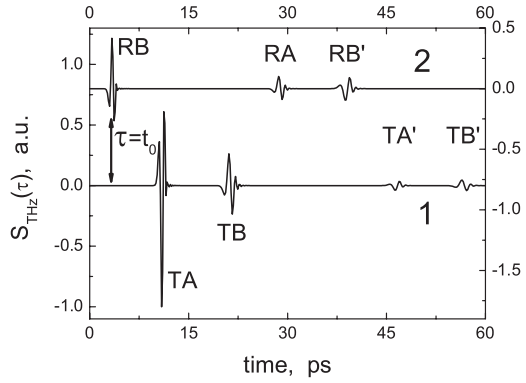

FIG. 3. Comparison of theoretical waveforms emitted forwardly (curve 1) and backwardly (curve 2) from the slab of $LiNbO_3$ of 1 mm thickness.

time of the THz pulse $2Ln_{\mathrm{THz}}/c_0$. Then, the arrival time of TA′ is $t_{A'} = Ln_{\mathrm{opt}}/c_0 + 2Ln_{\mathrm{THz}}/c_0$. This follows from both the experiments and theory—Fig. 2. To our knowledge, this striking result has not yet been reported elsewhere. It strongly favors the TR model, providing evidence for conversion of the polarization charge field into a pulse of THz radiation at the entry to and the exit from the slab. Moreover, Fig. 1 shows a striking inversion of the amplitude ratio from TA/TB $\gg 1$ to TA′/TB′ $\lesssim 1$, also in favor of this mechanism. It shows that after a seemingly simple round trip, THz radiation pulses demonstrate a striking change of amplitude ratio: compare the ratio of TA to TB′, and the ratio TA′ to TB′ in Fig. 1. Had the sources of pulses TA and TB been localized within the same spatial region of the nonlinear slab from the front surface, as interpreted in [1], then both TA and TB pulses would bounce back and forth keeping at least the same amplitude ratio. From the data of Fig. 3, we estimate the ratio of formation lengths for forward to backwards emitted THz radiation. The backward emitted pulses are shown by using "R" to mark their affiliation to the backward (reflection) direction. Since the field amplitude is proportional to the value of the formation-coherence length, we obtain the ratio $\eta = \mathrm{TB/RB} \sim L_{\mathrm{coh}}^{\mathrm{FW}}/L_{\mathrm{coh}}^{BW}$. It is clear that the ratio TA/TB is a measure of absorption in the slab. Assuming that the absolute value of peak amplitude remains the same on both interfaces, we recover the amplitude of the TB pulse at $z = 0 + \mathrm{TB}|_{z=0+} \sim \mathrm{TA}$. Then, from Fig. 3 we find $L_{\mathrm{coh}}^{\mathrm{FW}}/L_{\mathrm{coh}}^{\mathrm{BW}} \simeq 2.5$; this is in a good agreement with the calculated value of $\eta \approx 2.46$.

To summarize, the theory unambiguously establishes the location of sources of THz radiation to be in the regions, adjacent to the input and output interfaces, where the polarization charge is instantaneously formed and accelerated and subsequently instantaneously decelerated and extinguished. The experiments fully back up our theoretical conclusions. It can be shown that the interference of THz TR, emanating from both boundaries, causes the appearance of Maker fringes [3]. A more detailed account is published elsewhere.

The authors would like to acknowledge support from the Royal Society (U.K.) (visit grant for ASN); the Ministry of Education and Science of Armenia, Contracts No. 840; the Russian Foundation for Basic Research Grant No. 05-02-17770, and the grant for innovations support from the Russian Academy of Sciences.

*Electronic address: nick.zinovev@durham.ac.uk

[1] N. Bloembergen and P. S. Pershan, Phys. Rev. **128**, 606 (1962).
[2] J. A. Armstrong *et al.*, Phys. Rev. **127**, 1918 (1962).
[3] P. D. Maker *et al.*, Phys. Rev. Lett. **8**, 21 (1962).
[4] J. Jerphagnon and S. K. Kurtz, J. Appl. Phys. **41**, 1667 (1970).
[5] F. Zernike, Jr., and P. R. Berman, Phys. Rev. Lett. **15**, 999 (1965).
[6] J. Morris and Y. R. Shen, Opt. Commun. **3**, 81 (1971); K. H. Yang *et al.*, Appl. Phys. Lett. **19**, 320 (1971).
[7] T. Brabec and F. Krausz, Rev. Mod. Phys. **72**, 545 (2000).
[8] K. Wynne and J. J. Carey, Opt. Commun. **256**, 400 (2005).
[9] Y. J. Ding, Opt. Lett. **29**, 2650 (2004).
[10] G. A. Askar'yan, Sov. Phys. JETP **15**, 943 (1962) [Zh. Eksp. Teor. Fiz. **42**, 1360 (1962)].
[11] V. L. Ginzburg and V. N. Tsytovich, *Transition Radiation and Transition Scattering*, The Adam Hilger Series on Plasma Physics (Adam Hilger, Bristol and New York, 1990).
[12] D. H. Auston *et al.*, Phys. Rev. Lett. **53**, 1555 (1984).
[13] D. A. Kleinman and D. H. Auston, IEEE J. Quantum Electron. **20**, 964 (1984).
[14] D. H. Auston and M. C. Nuss, IEEE J. Quantum Electron. **24**, 184 (1988).
[15] L. Xu, X.-C. Zhang, and D. H. Auston, Appl. Phys. Lett. **61**, 1784 (1992).
[16] I. E. Tamm, J. Phys. (Moscow) **1**, 439 (1939).
[17] G. M. Afanasiev *et al.*, J. Phys. A **33**, 7585 (2000).
[18] B. M. Bolotovskii, Proc. (Tr.) P. N. Lebedev Phys. Inst. [Acad. Sci. USSR] **140**, 95 (1982).
[19] We point out that very often, e.g. [8,9], another set of BC, $E|_{z=0} = 0$ and $dE/dz|_{z=0} = 0$, is used to solve the radiation problem in a slab. It is worthwhile to note that such choice of BC is unreasonable as it causes serious artifacts such as zero backward emission from slab, etc.
[20] M. Born and E. Wolf, *Principles of Optics* (Pergamon, New York, 1970).
[21] Q. Wu and X.-C. Zhang, IEEE J. Sel. Top. Quantum Electron. **2**, 693 (1996).
[22] G. Gallot and D. Grischkowsky, J. Opt. Soc. Am. B **16**, 1204 (1999).
[23] A. S. Barker, Jr., and R. Loudon, Phys. Rev. **158**, 433 (1967).
[24] S. Kojima *et al.*, Phys. Status Solidi (c) **1**, 2674 (2004).
[25] In the experimental waveform it is followed by weak prolonged oscillations related to various specific spectroscopic details, such as the residual water absorption of the free space atmosphere, etc.